Archive of SID.ir

Journal of Applied Fluid Mechanics, Vol. 15, No. 2, pp. 453-464, 2022.
Available online at www.jafmonline.net, ISSN 1735-3572, EISSN 1735-3645.
https://doi.org/10.47176/jafm.15.02.33031

Inverse Design and Optimization of Low Specific Speed Centrifugal Pump Blade Based on Adaptive POD Hybrid Model

X. B. Chen[1], R. H. Zhang[1,2†] and W. F. Yang[1]

[1] *School of Energy and Power Engineering, Lanzhou University of Technology, Lanzhou, Gansu, 730050, China*
[2] *Key Laboratory of Fluid machinery and Systems, Lanzhou University of Technology, Lanzhou, Gansu, 730050, China*

†*Corresponding Author Email: zhangrh@lut.cn*

(Received May 21, 2021; accepted October 11, 2021)

ABSTRACT

To improve the prediction accuracy of the surrogate model and reduce the calculation cost for hydraulic optimization design of centrifugal pump impeller, an inverse design and optimization method based on adaptive proper orthogonal decomposition (APOD) hybrid model was proposed. Initial samples were designed by perturbing blade control parameters of the original model. The samples were classified using the K-means clustering algorithm, and the adaptive samples were selected according to the category of the objective sample. The snapshot set is composed of blade shape parameters and the CFD flow field data in impeller, which is decomposed into a linear combination of orthogonal bases by the proper orthogonal decomposition (POD) method to predict the objective parameters. According to the objective load distribution, the low specific speed centrifugal pump was inversely designed by using the APOD model, and its initial blade was obtained. And then, the flow field corresponding to disturbed blade shape was predicted using the APOD method, so as to evaluate the gradient of the objective function to design variables. Finally, the initial blade was optimized by the gradient descent method. The results show that the APOD hybrid model method can be employed to accomplish the blade inverse design and the flow field prediction in the optimization design of centrifugal impeller, which significantly reduces the numerical calculation cost and improves the accuracy of the flow field prediction.

Keywords: Proper orthogonal decomposition; Adaptive surrogate model; Inverse design; Optimization; Centrifugal pump.

NOMENCLATURE

a	blade shape parameter	q	geometry boundary
$\boldsymbol{b}$	inner product of a complete vector and POD basis vector	$\boldsymbol{R}$	position vector of points in blade surface
		S	suction side of blade
$\mathbf{C}$	design space	$\boldsymbol{U}$	snapshot sets
F	flow field parameter	$\boldsymbol{U}_1$	complete vector sets
f	blade load distribution	$\boldsymbol{u}$	incomplete vector
$\boldsymbol{G}$	left singular matrix	$\boldsymbol{V}$	right singular matrix
g	output parameter of RBF model	$\boldsymbol{v}$	design variable
H	rated head of pump	W	model coefficient of RBF
J	objective function	x	input parameter of RBF model
$\boldsymbol{K}$	inner product of POD basis vector	$\boldsymbol{\alpha}$	POD basis coefficient
L	number of grid points	β	blade angle
l	number of blade shape parameters	β_1	inlet angle of blade
M	torque of impeller	β_2	outlet angle of blade
m	number of iterations	$\boldsymbol{\Phi}$	POD basis vector
N	number of samples	ϕ	blade wrap angle
$\boldsymbol{n}$	normal vector of blade surface	ψ	Gaussian basis function
n	rotational speed	$\boldsymbol{\Sigma}$	diagonal matrix containing all eigenvalues
n_s	specific speed of impeller		

Archive of SID.ir

Archive of SID.ir

P	pressure side of blade	τ_w	tangential stress
p	pressure distribution	λ	scale factor
Q_d	rated flow of pump	η	rated efficiency of pump

1. INTRODUCTION

The optimization design of the centrifugal pump can also be considered as the problem of flow optimization. However, the complex relationship between geometric parameters and inner flow makes the research progress of pump optimization design slow (Derakhshan *et al*. 2013; Shim and Kim 2020; Zhang and Zhao 2020). The design of centrifugal pump blade mostly adopts the traditional one-dimensional and two-dimensional design theory. The design process is inconvenient, and the hydraulic performance of the pump is highly dependent on the designer's experience, so it is difficult to ensure that the designed pump has high performance. To solve this problem, many relevant and meaningful works have been carried out (Zangeneh *et al.* 1996; Tan *et al*. 2010; Tong *et al*. 2020; Han *et al*. 2020). Currently, the optimization design methods of centrifugal pumps mainly include the response surface optimization method based on experimental design (Kim *et al*. 2012; Wang *et al*. 2017), the intelligent optimization method based on evolutionary algorithm (Huang *et al*. 2015; Li *et al.* 2019), the gradient-based optimization method (Jameson 1988; Mohammadi 2010; Zhang *et al*. 2014). In the response surface optimization method and intelligent optimization method, the calculation cost increases exponentially with the increasing dimension of design variables. The main difficulty for the gradient optimization method is that the gradient vector for the objective function with respect to the design variables is hard to evaluate. The calculation cost also gradually increases with the increase in the dimension of the design variables. To reduce the calculation cost, Jameson (1988) proposed the adjoint method to optimize the aerodynamic shape. In each optimization iteration, the flow field and adjoint field need to be calculated only once. The calculation cost is significantly reduced, but the derivation of complex adjoint equations and boundary conditions is difficult. The incomplete sensitivities method (Mohammadi 2010) ignores the influence of geometric shape disturbance on the flow field when calculating the gradient of the objective function to design variables. Although the calculation cost is significantly reduced, the prediction accuracy of the objective function is reduced. Compared to the above-mentioned methods, the surrogate model can quickly determine the function responses corresponding to the given inputs with adequate accuracy. In this research, the surrogate model was applied respectively in the inverse design and optimization of centrifugal impeller.

The proper orthogonal decomposition (POD) (Chatterjee 2000), also known as Karhunen-Loeve (K-L) expansion or principal components analysis, is to determine a set of the optimal bases for the system through eigen decomposition and represent the complex data system as the inner product of a series of base vectors and corresponding basis coefficients. At present, the POD-based feature analysis method has been successfully applied to image processing (Sirovich and Kirby 1987), reduced-order model (Siddiqui *et al*. 2020), turbulence structure analysis (Holmes *et al*. 1996), and data mining (Duan *et al*. 2019; Zhang *et al*. 2021). POD is also widely used to fill the missing data, namely the Gappy POD method. Gappy POD is a surrogate model for filling missing data, which is usually used in inverse problem design, flow field reconstruction, and aerodynamics airfoil optimization (Buithanh *et al*. 2004; Luo *et al*. 2015; Qiu *et al*. 2018; Guo *et al*. 2019). Luo *et al*. (2015). proposed an iterative inverse design method based on Gappy POD and used it for the inverse design of turbine blades. Buithanh *et al*. (2004) used the Gappy POD method to effectively combine the experimental data with computational data and complete the inverse design and flow reconstruction for airfoils. Qiu *et al*. (2018) combined the POD-based data dimension reduction method with the global optimization method to form a new optimization system, aiming at improving the efficiency of traditional global optimization.

The fitting of the basis coefficient and the selection of samples have an important impact on the description accuracy of POD. In early applications, POD with linear regression, such as the least-squares method, was widely used to obtain the coefficients of POD basis modes. To improve the response accuracy of POD to a nonlinear system, Guénot *et al*. (2013) and Kato and Funazak (2014) proposed the POD-based method on use of the radial basis function (RBF), which was then used for aerodynamic shape optimization. Luo *et al*. (2017) introduced the POD-RBF hybrid model to reconstruct complex flow for the transonic blade, and then the aerodynamic optimization of the transonic compressor was carried out. These researches show that the expression ability of the POD-RBF hybrid model for the nonlinear system is significantly higher than that of POD with linear regression. For the selection of samples, the commonly used sampling methods are static sampling methods, which only focus on the distribution of samples in design variables space. The samples cannot dynamically adapt to the objective sample. In this paper, samples were classified according to their characteristics, and a dynamic adaptive sampling strategy was proposed, which was combined with the POD-RBF surrogate model to construct the adaptive proper orthogonal decomposition (APOD) hybrid model used in this study.

Archive of SID.ir

Archive of SID.ir

In this research, an APOD hybrid model was introduced to the inverse design and optimization of the centrifugal pump blade. The initial blade shape was obtained firstly by inverse design, and then the flow field corresponding to disturbed blade shape was reconstructed to predict the gradient of the objective function to design variables. The blade shape was optimized by the gradient descent method, and the optimal design of the centrifugal impeller was finally obtained.

2. ADAPTIVE PROPER ORTHOGONAL DECOMPOSITION (APOD) HYBRID MODEL

2.1 Principle of Gappy POD Method

Compared with the original POD, snapshot POD (Sirovich 1986) reduces the order of autocorrelation matrix to the number of snapshots, which significantly improves the effectiveness and stability of eigen decomposition. Gappy POD, an extension of snapshot POD, determines the basis modes of the data system by singular value decomposition (SVD). The basic principle of reconstructing missing data by Gappy POD was briefly introduced in the following.

Snapshot set $\boldsymbol{U}$ consists of the vector set $\boldsymbol{U}_1$ and $\boldsymbol{u}$, and the vectors in $\boldsymbol{U}_1$ and $\boldsymbol{u}$ correspond to each other:

$$\boldsymbol{U} = [\boldsymbol{U}_1 \ \boldsymbol{u}]^{\mathrm{T}}, \tag{1}$$

where all elements are completely known in vector set $\boldsymbol{U}_1$, but some elements in the incomplete vector $\boldsymbol{u}$ are missing:

$$\boldsymbol{u} = [\boldsymbol{u}_1 \ \boldsymbol{u}_2], \tag{2}$$

$$\Phi_i = [\Phi_{i,1} \ \Phi_{i,2}], \tag{3}$$

where $\boldsymbol{u}_1$ and $\boldsymbol{u}_2$ are the vector components consisting of the given data and the missing data, respectively; $\Phi_{i,1}$ and $\Phi_{i,2}$ are the corresponding POD basis. The missing data in vector $\boldsymbol{u}_2$ need to be filled.

The vector $\boldsymbol{u}_1$ is fitted by POD basis corresponding to the given data, i.e.

$$\boldsymbol{u}_{11} = \sum_{i=1}^{N} \alpha_i \Phi_{i,1}, \tag{4}$$

where $\boldsymbol{u}_{11}$ is the reproduced vector, which requires the smallest deviation from the originally given vector $\boldsymbol{u}_1$, N is the number of samples. The basis coefficient $\boldsymbol{\alpha}$ can be obtained by solving the least-squares problem:

$$\boldsymbol{K}\boldsymbol{\alpha} = \boldsymbol{b}, \tag{5}$$

where $\boldsymbol{K} = (\Phi_{i,1}, \Phi_{j,1})$ and $\boldsymbol{b} = (\boldsymbol{u}_1, \Phi_{i,1})$. Once the coefficients are obtained, the missing data can be reconstructed by

$$\boldsymbol{u}_{22} = \sum_{i=1}^{N} \alpha_i \Phi_{i,2}. \tag{6}$$

The unknown vectors $\boldsymbol{u}_2$ can be replaced by $\boldsymbol{u}_{22}$, and the missing data are filled.

Regarding the objective distribution of flow parameters as the known subvector, an inverse design can be achieved by filling up the missing subvector of blade shape. Similarly, flow reconstruction can be achieved by regarding the objective blade shape as the known subvector.

2.2 POD-RBF Surrogate Model

Since the least-squares method belongs to one of the linear response methods, its description accuracy is inadequate for complex nonlinear systems. In this study, to improve the description performance of Gappy POD on missing data reconstructions, nonlinear regression instead of the least-squares method is used in the subsequent blade inverse design and flow field prediction. Snapshot set $\boldsymbol{U}$ can be decomposed by SVD:

$$\boldsymbol{U} = \boldsymbol{G}\boldsymbol{\Sigma}\boldsymbol{V}^{\mathrm{T}} = \boldsymbol{G}\boldsymbol{\Phi}, \tag{7}$$

where $\boldsymbol{G}$ and $\boldsymbol{V}$ are orthogonal matrices, $\boldsymbol{\Sigma}$ is a diagonal matrix containing all eigenvalues. $\boldsymbol{G}$ is composed of coefficient vectors. The response surface can be established by regarding each POD basis coefficient vector as the outputs and the sample parameters as the inputs. In this study, RBF is used to construct the response surface model of POD basis coefficients:

$$g_{kj} = \sum_{i=1}^{N} W_{ij} \psi(x_k, x_i), \tag{8}$$

where g_{kj} is the j-th component of the k-th POD basis coefficient vector, W_{ij} is the model coefficient, x_i is an input parameter of the model, and $\psi(x_k, x_i)$ is the Gaussian basis function. The POD basis vectors of the snapshot sets can be obtained by Eq. (7). POD basis coefficients of the objective sample are predicted by the RBF model, and the objective parameters are reconstructed, according to Eq. (7).

2.3 APOD Hybrid Model Method

In the POD surrogate model approach, the prediction accuracy is highly dependent on the selection of the samples. The commonly used static sampling method only considers the distribution of samples in design variables space, ignoring the influence of the sample characteristics on the surrogate model. The prediction accuracy of the constructed surrogate model will be significantly improved if the characteristics of samples are in high agreement with those of the objective sample. The K-means algorithm (Yang *et al.* 2020) is a classical iteration clustering analysis method that is widely used, and it classifies data according to some similarity measurement criterion, which can classify data with high similarity into the same category. In this study, the initial samples are classified by the K-means clustering algorithm, and an adaptive sample selection strategy with dynamic sampling is established. Combined with the POD-RBF, the APOD hybrid model of the centrifugal pump is constructed. The principle and implementation of APOD hybrid model have already been introduced in reference (Chen *et al.* 2021), and its basic process can be summarized as follows:

Archive of SID.ir

Archive of SID.ir

(1) Get the initial sample set by appropriately disturbing the blade control parameters of the original model.
(2) Simulate the inner flow by the CFD method and get the blade pressure and load distribution of all samples.
(3) Classify the initial samples by the K-means clustering algorithm.
(4) Select the adaptive samples according to the category of the objective sample.
(5) Construct the POD hybrid model using adaptive samples.
(6) Predict the objective blade shape parameters in blade inverse problem or flow parameters in flow field reconstruction, respectively.

3. APOD HYBRID MODEL INVERSE DESIGN AND OPTIMIZATION METHOD FOR CENTRIFUGAL PUMP BLADE

The basic idea of inverse design is to change the blade shape to make the performance parameters of the designed blade as close to the given objective performance as possible. Buithanh *et al.* (2004) applied the POD method to airfoil inverse design and optimization. Zhang *et al.* (2017) applied Gappy POD to blade inverse design for the centrifugal pump inverse problem. In this research, the APOD hybrid model is used for the inverse design of the centrifugal pump blade. The design variable is defined as the blade load distribution, and the objective is to get the geometry shape that produces the corresponding objective load distribution. In hydraulic machinery, the change in the energy of fluid from the impeller inlet to the outlet determines the inner flow characteristics and hydraulic performances within the impeller. Therefore, the gradient of the total pressure distribution is directly defined as the blade load. The inverse design problem is to find the corresponding impeller geometry shape which would realize the objective blade load.

The snapshot vector contains the blade shape parameters and the blade load distribution, it can be expressed as

$$[a_{i,1} \quad a_{i,2} \quad \cdots \quad a_{i,l} \mid f_{i,1} \quad f_{i,2} \quad \cdots \quad f_{i,L}], \tag{9}$$

where a is the blade shape parameter, l is the number of blade shape parameters, f is the blade load distribution, and L is the number of grid points. For low specific speed centrifugal impeller, the circumferential angles of the blade shape at different radii were taken as the blade shape parameters.

When the objective load distribution is given, the APOD hybrid model proposed in Sec. 2.3 is used to predict the corresponding blade shape parameters, thereby completing the blade inverse design and obtaining the initial blade of the centrifugal pump impeller.

For a given load distribution, it cannot be guaranteed to be the optimal distribution. Therefore, in order to improve the hydraulic performance of the initial blade, its optimization design is carried out subsequently. The design variables include the blade outlet angle β_2 and blade wrap angle φ. The design objective is to improve the pump efficiency under the design flow rate condition, and the blade shape is optimized while the meridional plane of the impeller remains unchanged. In the present study, the optimization problem can be described as

$$\min. J(\boldsymbol{v}),\ \forall\ \boldsymbol{v} \in \mathbf{C}, \boldsymbol{v} = [\beta_2, \varphi], \tag{10}$$

where $\mathbf{C}$ is the design space. The torque M acting on the impeller is the optimization objective, which can be expressed as

$$M = \int_{P,S} [(\boldsymbol{R} \times \boldsymbol{n}) \cdot p + (\boldsymbol{R} \times \boldsymbol{\tau}_w) \cdot \cot\beta] \mathrm{d}s + \int_{\text{hub,shroud}} (\boldsymbol{R} \times \boldsymbol{\tau}_w) \cdot \cot\beta \mathrm{d}s, \tag{11}$$

where P and S are the pressure side and suction side of the blade respectively; the subscripts "hub" and "shroud" represent hub and shroud of impeller; $\boldsymbol{\tau}_w$ is the tangential stress; β is the blade angle; $\boldsymbol{n}$ is the normal vector of blade surface; $\boldsymbol{R}$ is the position vector of points in blade surface; p is the pressure distribution on the blade.

The centrifugal impeller is optimized by the gradient descent method, and its objective function J can be expressed as the function of controls parameters, blade shape parameters and flow field parameters,

$$J = J(v_i, q(v_i), F(q(v_i))), \tag{12}$$

where v_i is the design variable of blade shape, $q(v_i)$ is geometry boundary, and $F(q(v_i))$ is the flow field parameter.

According to the derivation rule of composite function, the gradient of the objective function to design variables can be expressed as:

$$\frac{\mathrm{d}J}{\mathrm{d}v_i} = \frac{\partial J}{\partial v_i} + \frac{\partial J}{\partial q}\frac{\partial q}{\partial v_i} + \frac{\partial J}{\partial F}\frac{\partial F}{\partial q}\frac{\partial q}{\partial v_i}. \tag{13}$$

In the optimization process, when the blade shape is renewed, i times of flow field calculation is required, where i is the dimension of the design variable. The calculation cost increases exponentially with the increase of the dimension of the design variables, which tends to cause the curse of dimensionality when the number of design variables is very large .

To reduce the calculation cost of optimization in the centrifugal pump and improve the prediction accuracy of the flow field, the APOD hybrid model for flow field reconstruction is constructed by using the sample blade shape parameters and corresponding flow field data. The model is used to predict the flow field under the perturbations of the blade shape in the impeller optimization instead of CFD method. According to Eq. (13), the optimal impeller can be obtained by calculating the torque gradient and renewing the blade shape along the negative direction of the gradient vector, i.e.

$$v_i^{m+1} = v_i^m - \lambda \frac{\mathrm{d}J}{\mathrm{d}v_i}, \tag{14}$$

Archive of SID.ir

Archive of SID.ir

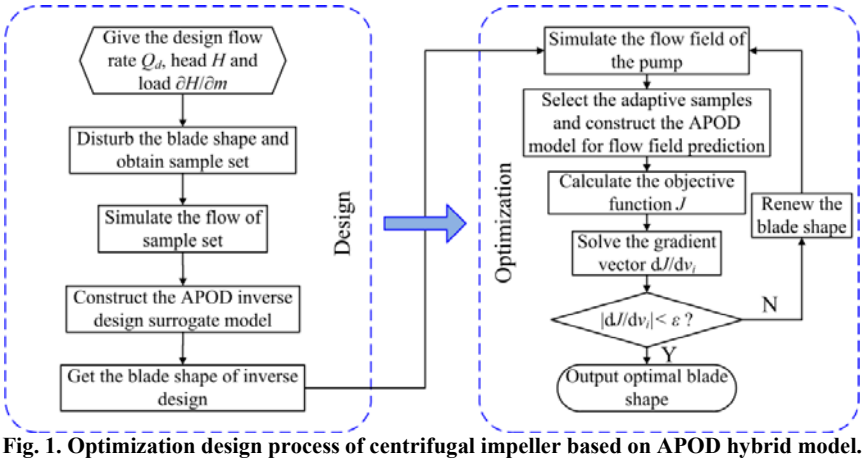


Fig. 1. Optimization design process of centrifugal impeller based on APOD hybrid model.

where λ is a scale factor, and m is the number of iterations.

In this study, a complete hydraulic optimization design framework for the design and optimization of the centrifugal impeller is established based on the proposed APOD hybrid model, and the basic flow process is shown in Fig. 1.

4. Results And Discussion

4.1 Numerical Calculation

A low specific speed centrifugal pump was applied to verify the inverse design and optimization method of centrifugal impeller based on the APOD hybrid model. Under the design condition, the flow rate Q_d of the pump is 12.5 m^3/h, the head H is 30.7 m, the efficiency η is 53 %, rotational speed n is 2900 r/min, and specific speed n_s ($n_s = 3.65n\sqrt{Q_d} / H^{0.75}$) is 48. The number of impeller blades is 4. The meridional plane and axial view of the impeller are shown in Fig. 2. The blade shape was parameterized by cubic Bezier curve, and the control parameters included inlet angle β_1, outlet angle β_2 and blade wrap angle φ. The value range of control parameters was determined according to the knowledge and experience of the centrifugal pump design, as shown in Table 1, in which the blade inlet angle β_1 does not change. In the experimental design of initial samples, in order to ensure that the blade shape does not appear S-shape, the blade outlet angle was designed to vary with the blade wrap angle. The blade outlet angle can be composed of the mean value $\overline{\beta}_2$ and the pulsation value β', where $\overline{\beta}_2$ and β' were related to the wrap angle φ as shown in Fig. 3. According to the design knowledge of the centrifugal pump, with the increase of the wrap angle, the corresponding $\overline{\beta}_2$ decreases, and the variation of $\overline{\beta}_2$ is relatively small near the two limit wrap angles that ensure the blade shape is smooth and does not appear S-shaped. Therefore, the relationship between $\overline{\beta}_2$ and the wrap angle satisfies the curve shown in Fig. 3(a). The blade outlet angle under the same wrap angle can also vary within a certain range, that is, the pulsation value β'. According to the relevant knowledge of impeller blade, when the blade wrap angle is 110°, the inlet and outlet angles of the blade are equal, so β' is 0°. When the blade wrap angle is far away from 110°, β' increases gradually. In this study, the maximum pulsation value is 5°, that is, the maximum value of β' is 5°. Therefore, the relationship between blade outlet angle pulsation value β' and wrap angle φ is shown in Fig. 3(b). Three different outlet angles, $\beta_2 = \overline{\beta}_2$, $\beta_2 = \overline{\beta}_2 + \beta'$ and $\beta_2 = \overline{\beta}_2 - \beta'$, can be taken for any wrap angle. According to the variation law of the above design parameters, the blade wrap angle was uniformly sampled from the value range of 80°-160° in this study. Therefore, within the value range of blade control parameters, 9 different wrap angles were selected to produce 25 sample models as the initial sample set for subsequent inverse design and flow field prediction surrogate model construction.

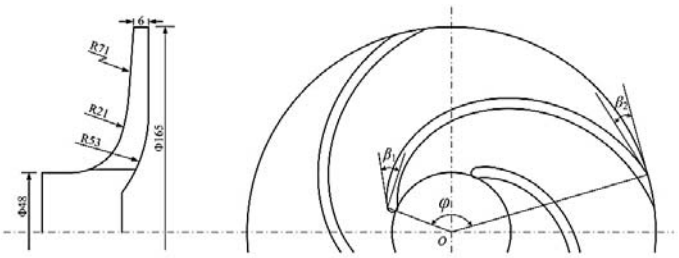


Fig. 2. Meridional plane and axial view of the prototype impeller.

Archive of SID.ir

Archive of SID.ir

Table 1 Range of blade shape control parameters

Parameters	Upper limits	Lower limits	Original
β_1	30°	30°	30°
β_2	50°	10°	17°
φ	160°	80°	143°

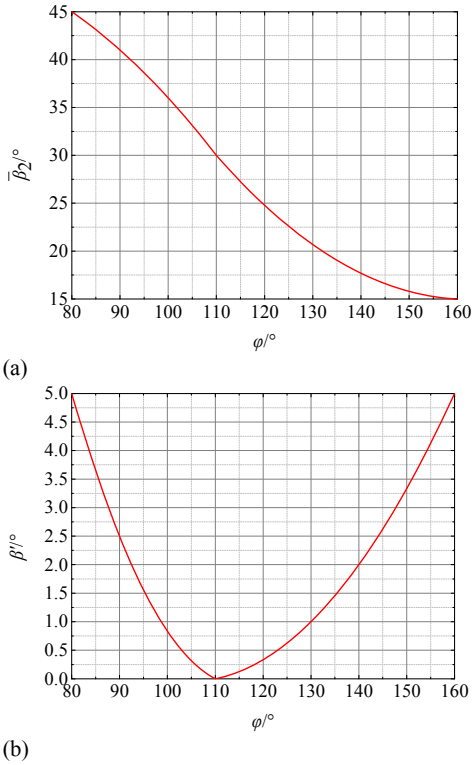


Fig. 3. Relationship between the blade outlet angle and blade wrap angle: (a) The relationship between $\bar{\beta}_2$ and φ; (b) The relationship between β' and φ.

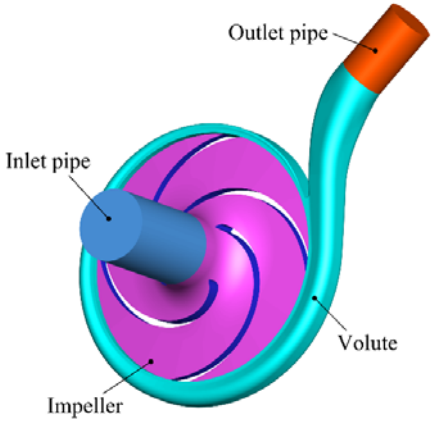


Fig. 4. Computational domain of the centrifugal pump.

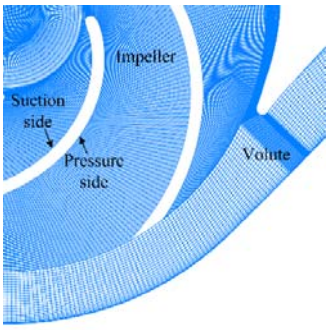


Fig. 5. Structured grid of impeller and volute.

The inner flow simulations of all samples in this study were solved with ANSYS Fluent CFD code. The flow was simulated by using RANS equations, and the SIMPLEC algorithm was used to couple pressure and velocity. The RNG k-ε turbulence model was adopted, and the near wall region was treated by standard wall functions. The velocity inlet and free outlet boundary conditions were specified, and all the solid walls were provided with a non-slip wall condition. The computational domain includes impeller, volute, inlet pipe, and outlet pipe, as shown in Fig. 4. The hexahedral structured meshes were employed to discretize the whole computational domain. The mesh of the impeller and volute is shown in Fig. 5. To balance simulation accuracy and the calculation cost, the grid independence test has already been introduced in previous work (Chen *et al*. 2021), and the total grid number was determined as about 1.3 million. The average y+ value near the wall in the whole numerical computational domain is 90, which meets the requirements of RNG k-ε turbulence model for the wall grid (Wang 2016).

The comparison of hydraulic performance between the experiment and the numerical simulation is shown in Fig. 6. The performance parameters of centrifugal pump are defined as:

$$H = \frac{p_{out} - p_{in}}{\rho g} + \Delta z \,, \tag{15}$$

where H is the head of the pump, p_{in} is the total pressure of the impeller inlet and p_{out} is the total pressure of the volute outlet.

$$\eta_h = \frac{\rho g Q H}{M\omega} \,, \tag{16}$$

where η_h is the hydraulic efficiency of the pump, Q is the flow rate, M is the torque of the pump and ω is angular velocity. Since only hydraulic loss is considered in numerical calculation, the total efficiency of the pump needs to be revised according to the empirical formulas of mechanical efficiency and volumetric efficiency. Therefore, the efficiency of numerical simulation is the product of hydraulic efficiency, volumetric efficiency and mechanical efficiency,

$$\eta = \eta_h \eta_v \eta_m \,, \tag{17}$$

Archive of SID.ir

Archive of SID.ir

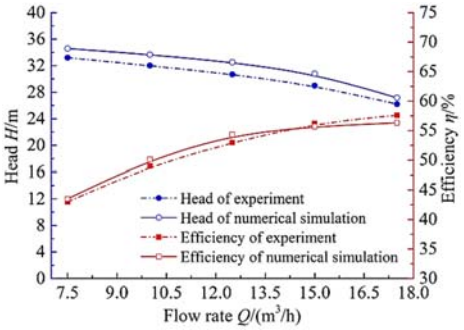


Fig. 6. Comparison of pump hydraulic performance between CFD and experiment.

where η_v is the volumetric efficiency and η_m is the mechanical efficiency, which can be calculated according to the empirical formulas (Pei *et al*. 2014).

As can be seen from Fig. 6, the trend of numerical calculations is consistent with the experimental results, and the values at different flow conditions are close. The maximum errors of the head and efficiency are 5.9% and 1.9%, respectively. Therefore, the numerical simulation is validated, and it can be applied in the following numerical calculation.

4.2 The Blade Inverse Design of Low Specific Speed Centrifugal Pump

According to the inverse design method of centrifugal impeller based on the APOD hybrid model proposed in Sec. 3, we can get the initial blade corresponding to the given objective load distribution. In this study, the load distribution of the original blade was taken as the objective load. The initial samples were classified using the K-means clustering algorithm based on the similarity of the blade load for the samples, and the classification results are shown in Fig. 7. The adaptive sample space was selected according to the objective load distribution, and then the APOD hybrid model of blade inverse design was constructed, and the initial blade was designed.

The inverse design of low specific speed centrifugal pump was carried out by the traditional fixed sample proper orthogonal decomposition (FPOD) hybrid model method and the APOD hybrid model method, respectively, and results are shown in Fig. 8. The inverse design blade obtained by the FPOD method has a certain deviation from the original blade, while the inverse design blade obtained by the APOD hybrid model method almost coincides with the original blade. The load distribution of the blade obtained by the two inverse problem methods was simulated by CFD and compared with the load distribution of the original blade, as shown in Fig. 9. It can be seen that the load distribution of the blade obtained by the FPOD hybrid model has a larger deviation from the load of the original blade, while the load distribution of the blade obtained by the APOD method is consistent with that of the original blade.

Figure 10 shows the comparison of the hydraulic performance between the blade designed by the APOD hybrid model and the original blade. As can be seen the performance of the inverse design blade agrees well with the original blade. Consequently, the prediction accuracy of the APOD hybrid model used in blade inverse design is significantly higher than that of FPOD, and the designed blade meets the given objective performance.

4.3 The Blade Optimization of Low Specific Speed Centrifugal Pump

To verify the prediction accuracy of the APOD hybrid model applied to the blade optimization for a low specific speed centrifugal pump, the flow field

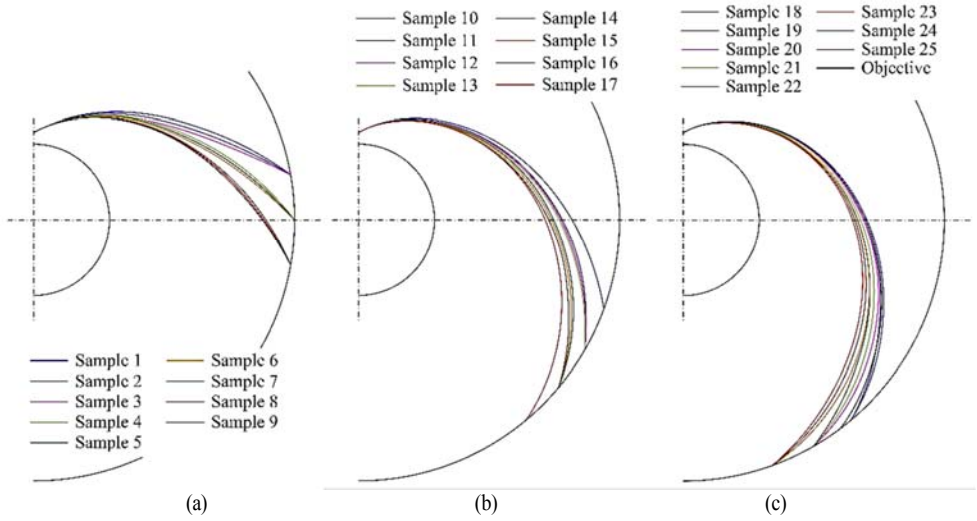


Fig. 7. Classification results of samples: (a) 1st category blade shapes; (b) 2nd category blade shapes; (c) 3rd category blade shapes.

Archive of SID.ir

Archive of SID.ir

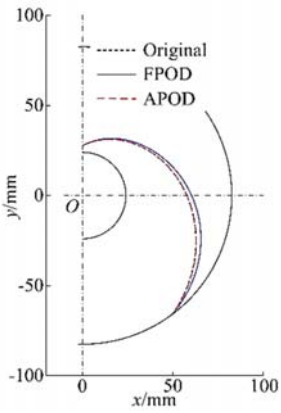


Fig. 8. Blade shape of inverse design.

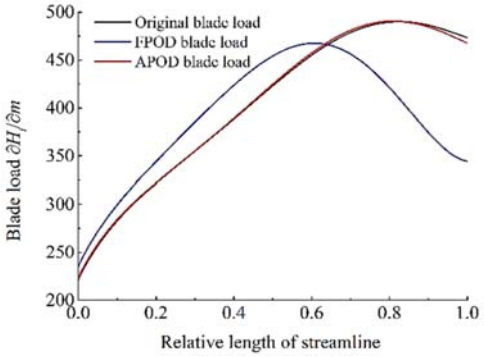


Fig. 9. Load distribution of inverse design blade.

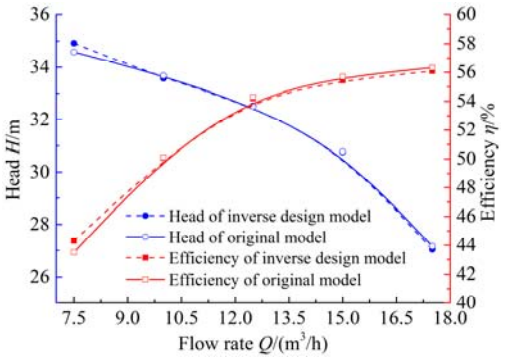


Fig. 10. Performance comparison between the inverse design model and the original model.

of the initial blade, that is, the inverse design blade obtained by APOD method in Sec. 4.2, was reconstructed. Contrary to the inverse problem, the flow field reconstruction is to predict the objective flow field (direct problem) by constructing a model under the given geometric parameters of the objective blade. According to the similarity of blade shape parameters for samples, the initial samples were classified again using the K-mean clustering algorithm, and the classification results were the same as those in the inverse design, as shown in Fig. 7. The adaptive samples were selected based on the objective blade shape parameters, and the APOD hybrid model of flow field reconstruction was constructed.

The pressure distribution of the initial blade was reconstructed by the FPOD and the APOD hybrid model, and compared with the pressure distribution calculated by CFD. The root mean square error (RMSE) of the POD prediction was calculated by using Eq. (18), and

$$\mathrm{RMSE}_i = \sqrt{\frac{1}{L}\sum_{i=1}^{L}\left(\frac{F_{i,POD}-F_{i,CFD}}{F_{i,CFD}}\right)^2}\times 100\%, \qquad (18)$$

where $F_{i,POD}$, $F_{i,CFD}$ were the flow field parameters predicted by POD and CFD, respectively and L is the number of grid points.

Figure 11 shows the comparison between the pressure distributions on the initial blade reconstructed by the two POD hybrid models and the CFD simulation results. It can be seen from Fig. 11(a) that the two POD models can predict the basic structure of the flow field, and the pressure gradually increases from the impeller inlet to the outlet. The predictions of the two surrogate models are close in most areas on the blade, and both are in agreement with the CFD calculation. In Fig. 11(b), the prediction error of the FPOD method is up to 5%. Compared with the FPOD model, the prediction result of the APOD hybrid method are closer to the CFD, and its prediction error is less than 2%, which has higher prediction accuracy. The RMSE of the FPOD hybrid model and APOD hybrid model for predicting the pressure distribution of the initial blade is 2.5% and 1.2%, respectively.

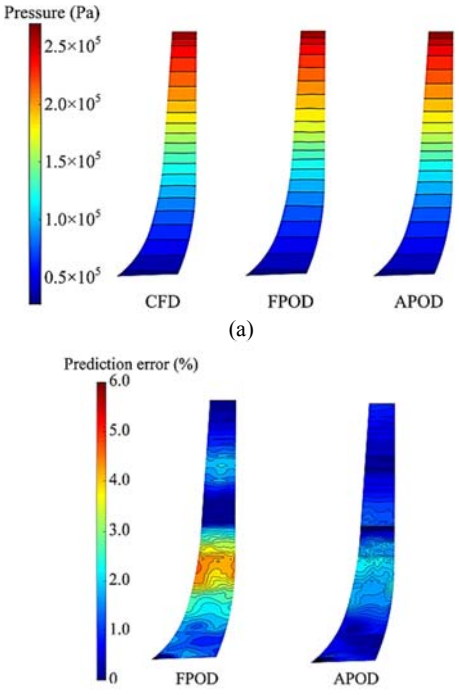


Fig. 11. Reconstruction of pressure on blade surface: (a) The pressure distributions of surrogate model prediction and CFD simulation; (b) Comparison of prediction error.

Archive of SID.ir

Archive of SID.ir

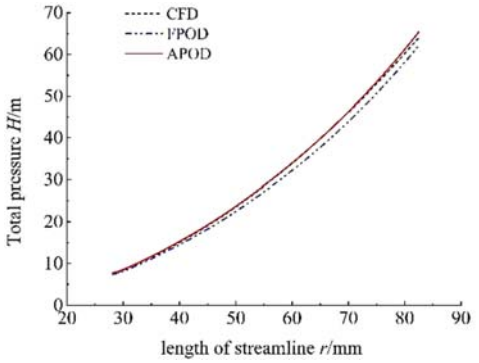


Fig. 12. Average total pressure distribution of shroud and hub on blade pressure side.

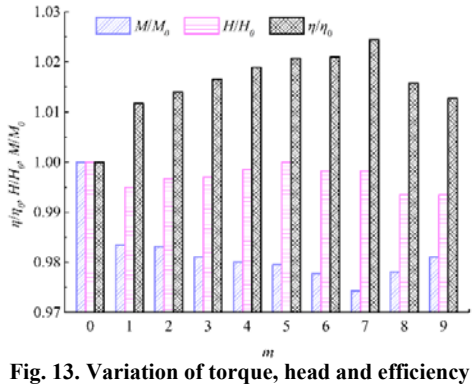


Fig. 13. Variation of torque, head and efficiency of pump in the process of optimization.

Figure 12 presents the comparison of the total pressure distribution on the blade pressure side between CFD calculation and surrogate model prediction, where the ordinate is the average value of total pressure on the blade shroud and hub. The changing trends of total pressure predicted by two POD methods show the same as that calculated by CFD. Compared with the FPOD hybrid model, the total pressure predicted by the APOD method is closer to that calculated by CFD. The RMSE of the FPOD method is 4.3%, while that of the APOD hybrid model is only 1.1%. Approximately 2 hours are needed to complete the simulation of the flow field in pump by CFD method on a DELL T620 workstation with 24 cores and 64 GB memory. However, it only needs 20 seconds by APOD method with the same workstation. It can be seen that the APOD hybrid model can quickly and accurately reconstruct the flow field in the centrifugal impeller. It is applied to predict the flow field response under the perturbations of the blade shape in the impeller optimization, which not only reduces the calculation cost of flow prediction but also improves the prediction accuracy of the surrogate model.

Figure 13 presents the variation of the hydraulic performance of the pump with the number of iterations during the optimization process, where M_0, H_0, and η_0 are the impeller torque, pump head and efficiency corresponding to the initial blade, respectively. As can be seen from this figure, with the increase of iteration number m, the impeller torque gradually decreases, and the efficiency of pump gradually increases. After 7 iterations, the pump efficiency reaches the maximum, and its head changes less compared with the initial design. In the next two iterations, the impeller torque increases gradually, the pump efficiency gradually decreases. Therefore, the result of the 7th iteration is taken as the final optimization result. Figure 14 shows the comparison between the optimized blade shape and the initial one. The optimized blade wrap angle φ is increased by 2˚, compared with the initial blade, and the blade outlet angle β_2 is reduced by 5˚.

The comparison of performance between the optimized and initial designs under different flow rate conditions is shown in Fig. 15. It can be seen that the efficiency of the optimized design is improved at

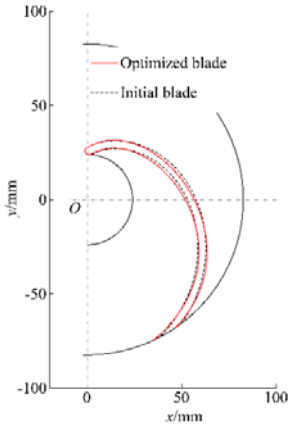


Fig. 14. Blade shapes of optimized design and initial design.

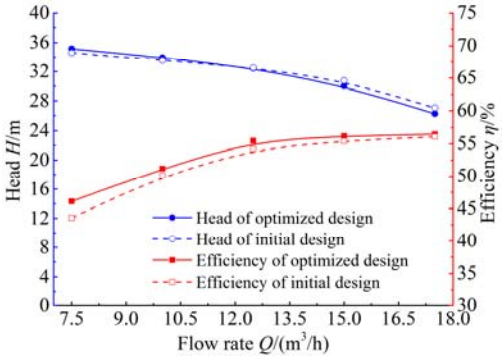
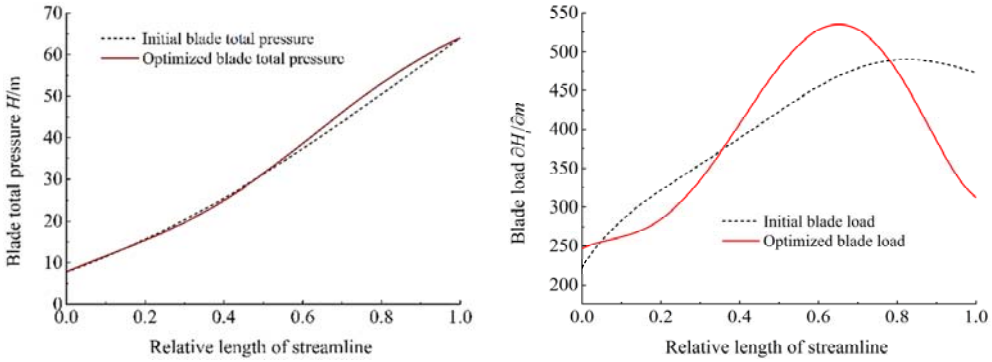


Fig. 15. Performance curves of optimized design and initial design.

all flow rate conditions. At the designed flow rate condition, the efficiency of the optimized design is improved by 1.27% compared with the initial design, and the head is basically unchanged. Comparing the performance curves of the optimized design and the initial design under low flow rate conditions, we can see that the head and efficiency of the pump are improved, in which the pump efficiency increases by 2.53% and the head increases by 0.55m at the $0.6Q_d$ (Q_d is the flow rate of pump under the design condition.). By comparing the efficiency and head under high flow rate conditions, it can be found that the pump efficiency has been improved, and the head

Archive of SID.ir

Archive of SID.ir



(a) (b)

Fig. 16. Load distributions of optimized blade and initial blade: (a) Total pressure curve; (b) Load curve.

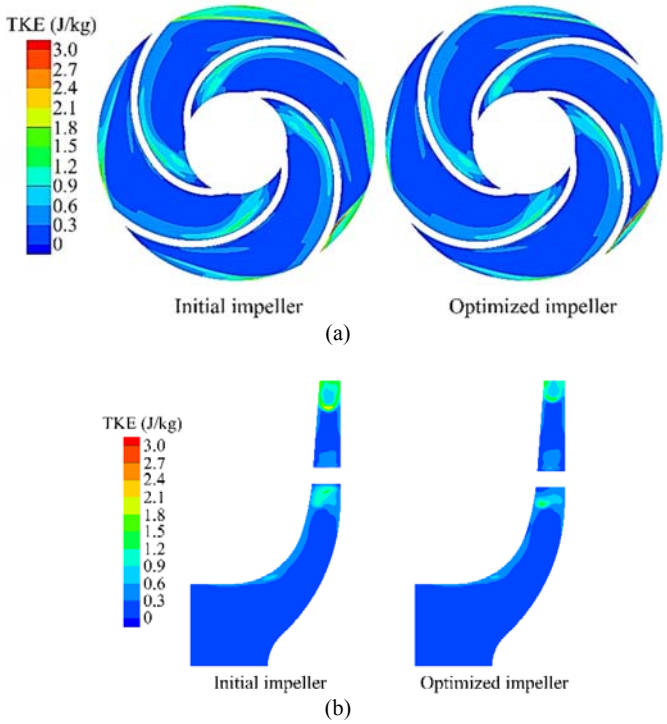


Fig. 17. Turbulent kinetic energy distributions of optimized impeller and initial impeller: (a) Middle plane of impeller; (b) Meridional plane of impeller.

has decreased slightly, with a decrease of less than 1.0m.

Figure 16(a) shows the total pressure distributions of the pressure side in the optimized blade and the initial blade. It can be seen from the figure that the total pressure distribution of the optimized blade near the outlet is larger than that of the initial blade. Figure 16(b) is the load distribution on the pressure side of the blade. We can see that the load of the optimized blade increases slowly near the inlet and increases rapidly after the relative streamline length of 0.2 compared to the initial blade. Moreover, the maximum load of the optimized blade moves forward, from the relative streamline length of 0.8 to the relative streamline length of 0.65. Compared with the initial blade, the load of blade outlet has a certain decrease, which is helpful to improve the stability of impeller outlet flow.

The turbulent kinetic energy (TKE) of the initial impeller and optimized impeller was compared and analyzed. Figure 17(a) shows the TKE in the middle plane of impeller. It can be seen from this figure that the TKE of the initial impeller is obviously larger at the impeller outlet and blade suction side. In contrast, the TKE in the flow passage of optimized impeller is lower. Figure 17(b) presents the TKE distribution in the meridional plane, we can also see that the value of TKE at the impeller outlet and blade suction side

Archive of SID.ir

Archive of SID.ir

decreases significantly after optimization. Combined with Figs. 14 and 17, it can be seen that appropriately increasing the blade wrap angle and reducing the blade outlet angle can significantly decrease the TKE in the impeller, which can make the flow in the impeller more stable and the hydraulic loss lower.

5. CONCLUSION

(1) An APOD hybrid model based on the K-means clustering algorithm was used for blade inverse design of low specific speed centrifugal pump. The inverse design results show that the blade designed by the APOD hybrid model method is coincident with the original blade, and the corresponding load distribution is consistent with the original blade load. Compared with the FPOD hybrid model, the prediction accuracy of the APOD model is significantly higher in the blade inverse design. Therefore, the proposed inverse design method of centrifugal pump blade is feasible.

(2) An optimization method of centrifugal impeller based on the APOD hybrid model was proposed. The flow field under the perturbations of the blade shape was accurately predicted using the APOD hybrid model. The accuracy of flow field prediction is significantly improved, and the calculated cost is greatly reduced in impeller optimization.

(3) The optimization results show that the efficiency of the optimized design is improved at all flow rate conditions. The efficiency of the optimized design is 1.27% higher than that of the initial design at the designed flow rate condition, and the head is basically unchanged. Further, the efficiency increase reaches 2.53% at the $0.6Q_d$, and the head of the pump increases 0.55m. The blade load distribution and flow structure in the impeller can be improved by increasing the blade wrap angle and decreasing the blade outlet angle.

ACKNOWLEDGEMENTS

This research was supported by Industrial Support Plan for Colleges and Universities in Gansu Province of China (Grant No. 2021CYZC-14) and National Natural Science Foundation of China (Grant No. 51979135).

REFERENCES

Buithanh, T., M. Damodaran and K. Willcox (2004). Aerodynamic Data Reconstruction and Inverse Design Using Proper Orthogonal Decomposition. *AIAA Journal* 42 (8), 1505–1516.

Chatterjee, A. (2000). An Introduction to the Proper Orthogonal Decomposition. *Current Science* 78 (7), 808–817.

Chen, X. B., R. H. Zhang, L. J. Jiang and W. F. Yang (2021). Adaptive POD surrogate model method for centrifugal pump impeller flow field reconstruction based on clustering algorithm. *Modern Physics Letters B* 35 (7), 2150126.

Derakhshan, S., M. Pourmahdavi, E. Abdolahnejad, A. Reihani and A. Ojaghi (2013). Numerical Shape Optimization of a Centrifugal Pump Impeller Using Artificial Bee Colony Algorithm. *Computers & Fluids* 81, 145–151.

Duan, Y. H., W. H. Wu, P. H. Zhang, F. L. Tong, Z. L. Fan, G. Y. Zhou and J. Q. Luo (2019). Performance Improvement of Optimization Solutions by POD-Based Data Mining. *Chinese Journal of Aeronautics* 32 (4), 826–838.

Guénot, M., I. Lepot, C. Sainvitu, J. Goblet and R. F. Coelho (2013). Adaptive Sampling Strategies for Non-Intrusive POD-Based Surrogates. *Engineering Computations* 30 (4), 521–547.

Guo, G. Q., R. H. Zhang, X. B. Chen and R. N. Li (2019). Optimization method for low specific speed centrifugal impeller based on POD surrogate model. *Journal of Huazhong University of Science and Technology (Natural Science Edition)* 47 (7), 50–55.

Holmes, P., J. L. Lumley and G. Berkooz (1996). *Turbulence, Coherent Structures, Dynamical Systems and Symmetry*. London, UK: Cambridge University Press.

Huang, R. F., X. W. Luo, B. Ji, P. Wang, A. Yu, Z. H. Zhai and J. J. Zhou (2015). Multi-Objective Optimization of a Mixed-Flow Pump Impeller Using Modified NSGA-II Algorithm. *Science China Technological Sciences* 58 (12), 2122–2130.

Han, X. D., Y. Kang, J. P. Sheng, Y. Hu and W. G. Zhao (2020). Centrifugal Pump Impeller and Volute Shape Optimization Via Combined NUMECA, Genetic Algorithm, and Back Propagation Neural Network. *Structural and Multidisciplinary Optimization* 61 (1), 381–409.

Jameson, A. (1988). Aerodynamic Design via Control Theory. *Journal of Scientific Computing* 3 (3), 233–260.

Kim, J. H., K. T. Oh, K. B. Pyun, C. K. Kim, Y. S. Choi and J. Y. Yoon (2012). Design Optimization of a Centrifugal Pump Impeller and Volute Using Computational Fluid Dynamics. *IOP Conference Series: Earth Environmental Science* 15, 032025.

Kato, H. and K. I. Funazak (2014, June). POD-Driven Adaptive Sampling for Efficient Surrogate Modeling and Its Application to Supersonic Turbine Optimization. In *Proceedings of ASME Turbo Expo 2014: Turbine Technical Conference and Exposition*, Düsseldorf, Germany.

Luo, J. Q., X. Tang, Y. H. Duan and F. Liu (2015, June). An Iterative Inverse Design Method of Turbomachinery Blades by Using Proper Orthogonal Decomposition. In *Proceedings of ASME Turbo Expo 2015: Turbine Technical*

Archive of SID.ir

Archive of SID.ir

Conference and Exposition, Montreal, Canada.

Luo, J. Q., Y. L. Zhu, X. Tang and F. Liu (2017). Flow Reconstructions and Aerodynamic Shape Optimization of Turbomachinery Blades by POD-Based Hybrid Models. *Science China Technological Sciences* 60 (11), 1658–1673.

Li, X. J., Y. J. Zhao and Z. X. Liu (2019). A Novel Global Optimization Algorithm and Data-Mining Methods for Turbomachinery Design. *Structural and Multidisciplinary Optimization* 60 (2), 581–612.

Mohammadi, B. (2010). Hadamard Incomplete Sensitivity and Shape Optimization. *Control and Cybernetics* 39 (3), 615–626.

Pei, J., W. J. Wang and S. Q. Yuan (2014). Statistical Analysis Of Pressure Fluctuations During Unsteady Flow For Low-Specific-Speed Centrifugal Pumps. *Journal of Central South University* 21 (3), 1017–1024.

Qiu, Y. S., J. Q. Bai, N. Liu and C. Wang (2018). Global Aerodynamic Design Optimization Based on Data Dimensionality Reduction. *Chinese Journal of Aeronautics* 31 (4), 643–659.

Sirovich, L. (1986). Turbulence and the Dynamics of Coherent Structures. Part I: Coherent Structures. *Quarterly of Applied Mathematics* 45 (3), 561–571.

Sirovich, L. and M. Kirby (1987). Low-Dimensional Procedure for the Characterization of Human Faces. *Journal of the Optical Society of America A* 4 (3), 519–524.

Shim, H. S. and K. Y. Kim (2020). Design Optimization of the Impeller and Volute of a Centrifugal Pump to Improve the Hydraulic Performance and Flow Stability. *ASME Journal of Fluids Engineering* 142 (10), 101211.

Siddiqui, M. S., S. T. M. Latif, M. Saeed, M. Rahman, A. W. Badar and S. M. Hasan (2020). Reduced Order Model of Offshore Wind Turbine Wake by Proper Orthogonal Decomposition. *International Journal of Heat and Fluid Flow* 82, 108554.

Tan, L., S. L. Cao, S. B. Gui and B. S. Zhu (2010). Centrifugal pump impeller inverse design by using direct inverse problem iteration. *Transactions of the Chinese Society of Agricultural Machinery* 41 (7), 30–35.

Tong, S. G., H. Zhao, H. Q. Liu, Y. Yu, J. F. Li and F. Y. Cong (2020). Multi-Objective Optimization of Multistage Centrifugal Pump Based on Surrogate Model. *ASME Journal of Fluids Engineering* 142 (1), 011101.

Wang, F. J. (2016). Research Progress of Computational Model for Rotating Turbulent Flow in Fluid machinery. *Transactions of the Chinese society for Agricultural Machinery* 47 (2), 1–14.

Wang, C., W. D. Shi, X. K. Wang, X. P. Jiang, Y. Yang, W. Li and L. Zhou (2017). Optimal Design of Multistage Centrifugal Pump Based on the Combined Energy Loss Model and Computational Fluid Dynamics. *Applied Energy* 187, 10–26.

Yang, W., H. Long, L. H. Ma and H. F. Sun (2020). Research on Clustering Method Based on Weighted Distance Density and K-means. *Procedia Computer Science* 166, 507–511.

Zangeneh, M., A. Goto and T. Takemura (1996). Suppression of Secondary Flows in a Mixed-Flow Pump Impeller by Application of Three-Dimensional Inverse Design Method: Part 1-Design and Numerical Validation. *Journal of Turbomachinery* 118 (7), 536–542.

Zhang, R. H., M. Guo, J. H. Yang and Y. Liu (2014). Blade shape optimization of centrifugal pump impeller with adjoint method. *Journal of Drainage and Irrigation Machinery Engineering* 32 (11), 943–947.

Zhang, R. H., R. Guo, J. H. Yang, and J. Q. Luo (2017). Inverse Method of Centrifugal Pump Impeller Based on Proper Orthogonal Decomposition (POD) Method. *Chinese Journal of Mechanical Engineering* 30 (4), 1025–1031.

Zhang, R. H. and X. T. Zhao (2020). Inverse Method of Centrifugal Pump Blade Based on Gaussian Process Regression. *Mathematical Problems in Engineering* 2020, 4605625.

Zhang, R. H., X. B. Chen and J. Q. Luo (2021). Knowledge Mining of Low Specific Speed Centrifugal Pump Impeller Based on Proper Orthogonal Decomposition Method. *Journal of Thermal Science* 30, 840–848.

Archive of SID.ir